



## NRC Publications Archive Archives des publications du CNRC

### **Traction, forces, wheel climb and damage in high-speed railway operations**

Magel, Eric; Tajaddini, Ali; Trosino, Michael; Kalousek, Joe

This publication could be one of several versions: author's original, accepted manuscript or the publisher's version. / La version de cette publication peut être l'une des suivantes : la version prépublication de l'auteur, la version acceptée du manuscrit ou la version de l'éditeur.

For the publisher's version, please access the DOI link below. / Pour consulter la version de l'éditeur, utilisez le lien DOI ci-dessous.

#### **Publisher's version / Version de l'éditeur:**

<https://doi.org/10.1016/j.wear.2008.01.036>

*Wear*, 256, 9-10, pp. 1446-1451, 2008-05-23

#### **NRC Publications Record / Notice d'Archives des publications de CNRC:**

<https://nrc-publications.canada.ca/eng/view/object/?id=19c568a7-7b6b-4604-bbb4-49c2154135ea>

<https://publications-cnrc.canada.ca/fra/voir/objet/?id=19c568a7-7b6b-4604-bbb4-49c2154135ea>

Access and use of this website and the material on it are subject to the Terms and Conditions set forth at

<https://nrc-publications.canada.ca/eng/copyright>

READ THESE TERMS AND CONDITIONS CAREFULLY BEFORE USING THIS WEBSITE.

L'accès à ce site Web et l'utilisation de son contenu sont assujettis aux conditions présentées dans le site

<https://publications-cnrc.canada.ca/fra/droits>

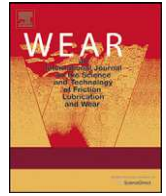
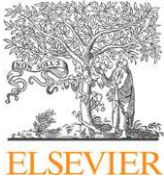
LISEZ CES CONDITIONS ATTENTIVEMENT AVANT D'UTILISER CE SITE WEB.

**Questions?** Contact the NRC Publications Archive team at

PublicationsArchive-ArchivesPublications@nrc-cnrc.gc.ca. If you wish to email the authors directly, please see the first page of the publication for their contact information.

**Vous avez des questions?** Nous pouvons vous aider. Pour communiquer directement avec un auteur, consultez la première page de la revue dans laquelle son article a été publié afin de trouver ses coordonnées. Si vous n'arrivez pas à les repérer, communiquez avec nous à PublicationsArchive-ArchivesPublications@nrc-cnrc.gc.ca.





# Traction, forces, wheel climb and damage in high-speed railway operations

Eric Magel<sup>a,\*</sup>, Ali Tajaddini<sup>b</sup>, Michael Trosino<sup>c</sup>, Joe Kalousek<sup>d</sup>

<sup>a</sup> Centre for Surface Transportation Technology, Canada

<sup>b</sup> Federal Railroad Administration, USA

<sup>c</sup> Amtrak, USA

<sup>d</sup> Consultant, Canada

## ARTICLE INFO

### Article history:

Accepted 22 January 2008

Available online 23 May 2008

### Keywords:

Traction coefficient

Friction

Adhesion

Wheel climb

Instrumented wheelset

High speed rail

## ABSTRACT

This paper summarizes the analysis of roughly 6 h of data from four instrumented wheelsets running at speeds of up to 240 km/h on the same Amtrak Acela trainset. Comparisons are made between power car and coach car traction values,  $L/V$  ratio, and damage (wear and RCF). The propensity for wheel climb is found to be roughly the same for power car and coach car wheels. The wear and RCF damage, as evaluated through the  $T\gamma$  index, is about 50% higher for the two power car wheelsets than for the two coach car wheelsets. The peak traction coefficient on the Amtrak system is measured to have a value of about 0.65 at low speeds, declining to about 0.22 at 200 km/h. These levels are much higher than those found in the literature for high-speed trains.

© 2008 Eric Magel. Published by Elsevier B.V. All rights reserved.

## 1. Introduction

Understanding creepage and forces at the wheel/rail interface is an ongoing quest for many contact mechanists. Increasingly elaborate models of vehicles, track, wheel/rail contact, materials and interfacial layers are being developed to evaluate the wheel/rail forces and thereby explain the phenomena of corrugation, wear, contact fatigue, hunting, noise, vibration and other wheel/rail issues. But often this work takes place without the benefit of field data for the model validation.

The last decade has seen a proliferation of devices for analyzing wheel/rail performance, with lateral force detectors, angle-of-attack systems and ride-quality meters proving particularly useful in measuring vehicle–track performance. But for studies of wheel/rail contact, arguably the most useful investigative tool is the instrumented wheelset or IWS.

## 2. The instrumented wheelset

To make an IWS system, the wheel plate of an otherwise standard wheelset is machined to remove as much excess metal as possible, i.e. remove stiffness from the system and make the wheels as flexible as possible within the bounds of safe operation. Finite element analysis of the resulting wheel is used to obtain a strain

map of the plate and identify the appropriate locations for strain measurements. Strain gauges are applied to the inside and outside of the wheel plate and hub (Fig. 1) for measuring the vertical, lateral and torque values for each wheel. The strain bridges are properly connected and then wired through a hole in the axle to a spinning amplifier mounted on the axle end. The signals are transferred from the axle to the carbody through a multi-channel slip ring device.

Eleven channels of data are collected per wheel (four lateral, two vertical, four position and one torque). Data are collected at 500 Hz, analogue filtered at 100–125 Hz and then digitally filtered in the software at 25 Hz. The data includes the vertical load, lateral load, wheel torque and lateral position of the contact patch with respect to the wheelset tapping line for each of the left and right wheel. The resulting signals show considerable “noise” which may or may not be real. For the purposes of this work, we “smoothed” the initial waveforms using a moving average of 100 points (0.2 s) and then extracted every 500th point (i.e. 1 point/s). This resulted in a data set of over 20,000 points for subsequent analysis.

The instrumented wheelset has seen a large number of applications including derailment investigations (e.g. [1]), studies to understand or validate track geometry standards [2,3], and measurements of bogie performance characteristics [4] often to compare modeling results with the measured forces. But with a few exceptions (e.g. [5–8]) the instrumented wheelset is generally not available to most researchers of the vehicle/track interaction. It is (currently) a relatively expensive tool to own or rent, and deployment is often onerous. But if the forces at the wheel/rail contact are to be measured, it is really the only method currently available.

\* Corresponding author.

E-mail address: [eric.magel@nrc-cnrc.gc.ca](mailto:eric.magel@nrc-cnrc.gc.ca) (E. Magel).



**Fig. 1.** Strain gauges placed on both sides of the wheel plate are used to measure strains which are then converted into vertical, lateral and longitudinal forces at the wheel/rail contact. A protective coating is applied over the gauges prior to deployment.

The high-speed Acela trains running on Amtrak’s Northeast Corridor are required each year to undergo a re-qualification test to ensure that with wear and time, the assembly of components continues to operate safely. These tests include simultaneous measurements from four instrumented wheelsets—in this case two in a (non-tilting) power car and two in the adjacent (tilting) coach car (Fig. 2). This 800 km run from Washington through New York and onwards to Boston is performed at speeds up to 240 km/h and (on a test basis) up to 225-mm cant deficiency. Under a program supported by the US Federal Railroad Administration, the IWS data provided by Amtrak from these four wheelsets is being analyzed to investigate a range of parameters having relevance to wheel–rail performance, modeling and testing. These include:

- (A) The available adhesion at speeds ranging from 10 to 240 km/h. This is calculated primarily through evaluation of the net tractive force measured at the low wheel in curving where the creep force may be saturated. The possible influence of thermal and dynamic effects on the wheel/rail interfacial layer will be considered.
- (B) The impact of braking and accelerating tractions. Their implications with respect to wear modeling, contact fatigue, lateral forces and wheel climb are discussed.
- (C) The effect of cant deficiency on the longitudinal and lateral tractions in both the leading and trailing axles. The vectorial resultant of the creepage vector is considered in light of RCF crack generation and orientations observed in the field.

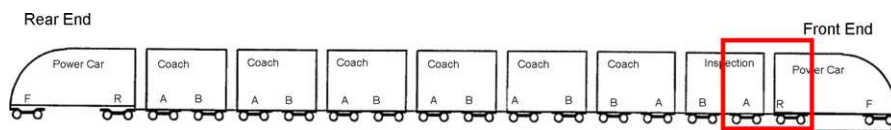


**Fig. 2.** An Acela train consists of power cars on each end with six, non-powered coach cars in between. For this test, Amtrak’s high-speed inspection coach (10003) was inserted in the consist. The trailing bogie of the power car and lead bogie of the inspection car were all equipped with instrumented wheelsets.

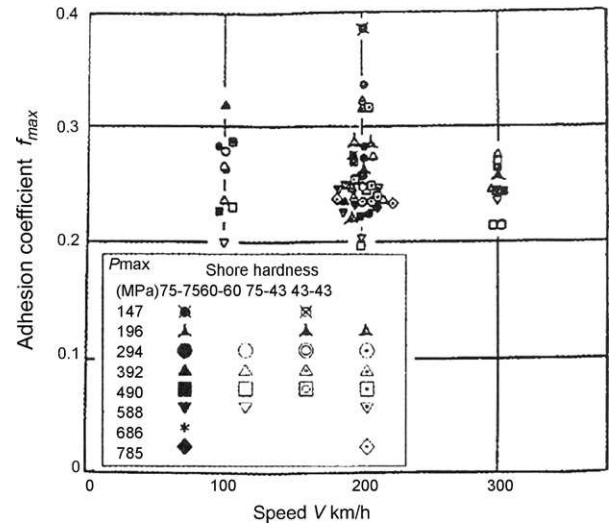


**Fig. 3.** Adhesion as a function of speed under dry conditions from Japan with a rail-roller rig [12].

### 3. Wheel/rail adhesion at high speed

#### 3.1. Review

The adhesion between wheel and rail has been noted by Godet and others [9,10] to be highly dependent on the characteristics of the interfacial layer and the amount of moisture present. But the effect of speed on the interfacial layer is not clear. One suggestion is that with increasing speeds, thermal conditions modify the strength properties of the interfacial layer, decreasing its shear strength and reducing the available wheel–rail friction [11]. Various roller rig and field measurements have shown mixed results. Adhesion testing with a large-scale rail/roller rig under dry conditions found no effect of speed on the traction/creepage curve (Fig. 3)—though there was a large variation in measured values attributed to the chemistry of the surface films on the components [12]. Testing in China on a high-speed roller rig found the same strong effect of speed on adhesion for the water contaminated interface but unfortunately, limitations in the rig allowed dry testing only to 70 km/h [13] and a statement again that the dry adhesion is little affected by speed. These results contrast with European field tests in the 1980s with a “tribo-train” that produced a series of curves for adhesion based on “very limited” data (Fig. 4A). They suggested that the decline in adhesion with speed depends on the suspension characteristics and “wheel–rail dynamic interaction” [14]. A traction performance design curve based on roller rig testing is employed in China [13] that closely matches the European field measurements.

#### 3.2. Analyzing the IWS data for adhesion

##### 3.2.1. Tangent running

In quasi-static tangent running the component of traction associated with low levels of spin creep can be ignored and adhesion

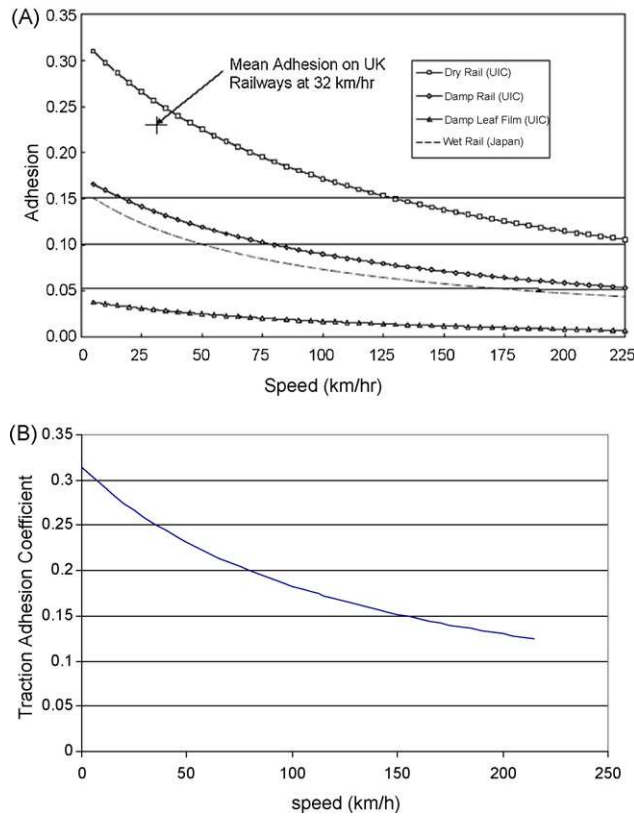


Fig. 4. (A) Adhesion coefficient measured on UK railways [14]. (B) Design adhesion–traction characteristic for high-speed trains, based on roller rig testing [13]. The design curve matches closely to the dry rail (UIC) measurements.

is then represented entirely by the longitudinal force measured by the wheelset divided by the wheelset vertical load. Fig. 5 plots the several thousand such events against the UK tribometer measurements and the design-performance curve from China. The upper envelope of the measured values mimics the shape of the Acela power car traction curve, showing steady traction performance to about 80 km/h and then rolling off at constant power beyond that point. The traction values under braking show the same general

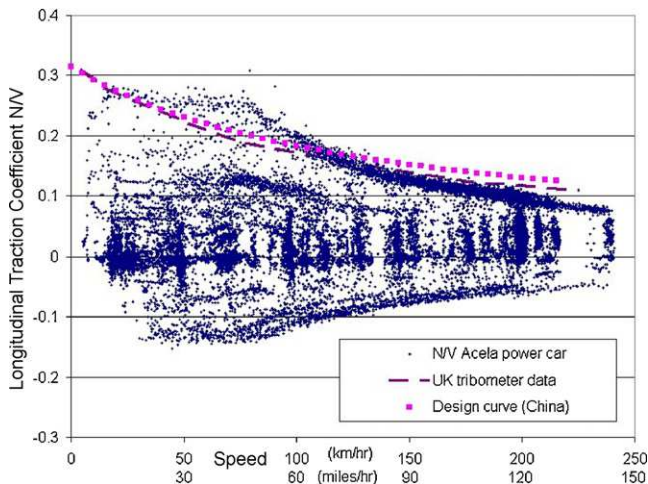


Fig. 5. Longitudinal traction coefficient for the leading axle of the power car.

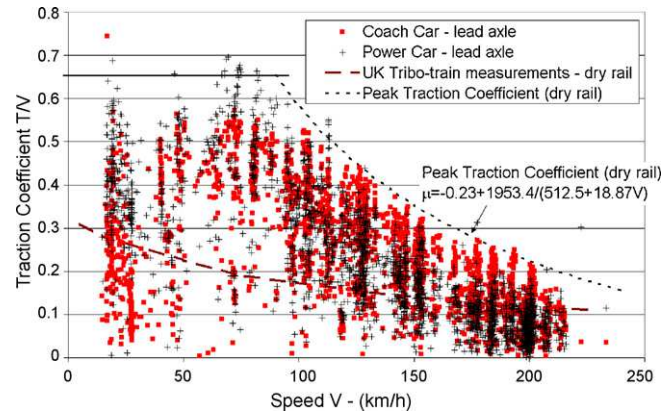


Fig. 6. Measured traction coefficient (includes lateral and longitudinal creep components) at the low wheel of the leading axle on the (non-powered) coach car and power car wheelsets through more than 600 curves on Amtrak's Northeast Corridor.

feature and are consistent with the regenerative braking capability of the Acela power car.

### 3.2.2. Traction coefficient in curves

Wheel/rail adhesion, or the traction coefficient is the ratio of the effective creep force divided by the normal load at the contact patch. In curves, creepage includes longitudinal, lateral and spin components [15]. But the instrumented wheelset measures the resultant of all forces, not just those due to creepage. The lateral force on the wheelset, for example, includes also the gravitational force that arises due to the plane of contact not being parallel to track level. The wheelset vertical load thus applies a lateral component of force to the rail (even in a frictionless environment) that is picked up by the wheelset. Since it is very difficult to know the contact angles at the high rail, we will consider only the low rail contact, where the 1:40 taper of the lightly worn instrumented wheelset is a fair presumption for the low rail contact angle.

The values for the measured low-rail traction coefficient through more than 600 curves are plotted against the train speed in Fig. 6. This figure shows all the traction values as they happen—some will be on the linear portion of Kalker traction–creepage curve (Fig. 7), some at peak (saturated creepage) and a few past the saturation creepage. The peak of traction–creepage curve is strongly affected by rail contamination, such as moisture and oily fluids and so in some locations (e.g. over lubricated curves) or under different environmental conditions (e.g. humidity, rain, snow, temperature) the peak levels measured can be quite different. The outside envelope of traction values shown in Fig. 6 represents the peak traction level measured on that day 13 April 2005 when the rail was dry and relatively uncontaminated.

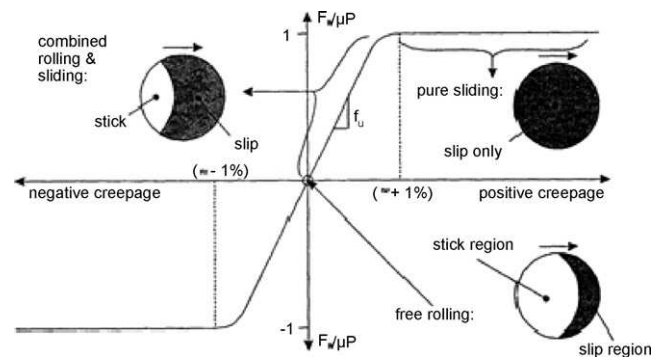


Fig. 7. The traction–creepage relationship [16].

Using the design adhesion formula from Ref. [13]:

$$\mu = k + \frac{c_1}{c_2 + c_3 V}$$

and fitting to several points representing the outside limits of the distribution, we arrive at a relationship for the peak traction coefficient available on the Amtrak Northeast Corridor under dry conditions by setting  $k = -0.23$ ,  $c_1 = 1953.4$ ,  $c_2 = 512.5$  and  $c_3 = 18.87$ , for speed  $V$  between about 100 and 200 km/h.

### 3.2.3. Discussion

The peak traction coefficients measured in curving (Fig. 6) are much higher than those in tangent running (Fig. 5). In straight line running the peak traction coefficient is clearly limited by the capabilities of the Acela propulsion system at high speeds. But in curving, the propulsion forces are supplemented by creep forces that arise from curving. The IWS measured peak values are 2–3 times greater than those values measured in Europe under dry conditions and saturated creepage (Fig. 4A).

Under conditions of dry rail and slow speed, the peak adhesion level of about 0.65 is the same as it would be for any heavy haul or mass transit system. The drop in the peak traction coefficient above about 90 km/h is consistent with experience elsewhere (Fig. 4) and is given by the curve fit shown in Fig. 6.

These results are clearly relevant to any modeling effort. The most detailed of vehicle and track models can be developed for important modeling work but often only simple assumptions made for the friction coefficient. But these same models will show that RCF, wear and various vehicle-track dynamics issues are quite sensitive to the friction conditions applied.

Whereas it is common to employ a peak friction coefficient of about 0.4–0.5, the IWS measurements of Fig. 6 show that higher values than these can occur. For wheel–rail damage and dynamics evaluations, one has to take the actual peak traction values (COF) that would be applicable. Using those reported by the UIC measurements or the various performance design curves will not properly bound the problem.

### 3.3. Numerical modeling

Dynamic modeling of the mild curve at Aberdeen Maryland was undertaken to determine at what friction coefficient the lateral and longitudinal force would match the measured data. We considered the Acela trainset negotiating the 1750 m radius curve at a steady 200 km/h and cant deficiency of 118 mm. We used smooth track geometry and only one set of rail profiles. Dynamic action of the wheelsets made it difficult to compare the IWS and quasi-static modeling results precisely. It could only be said that in order to get reasonable agreement, the friction coefficient most certainly needed to be less than 0.3—which is consistent with the value of about 0.2 in Fig. 6. Interestingly, the agreement improves if the gage-face friction is set to a value lower than the top-of-rail. It is not surprising that this might be so—quasi-static analysis shows that the creepage conditions differ dramatically at the gage-face and top-of-rail. In the case of the two-point high-rail contact, the vectorial sum of longitudinal and lateral creepage is about 0.18% at the top-of-rail and about 4% at the gage face. It seems likely that although both gage-face and top-of-rail are essentially dry at this curve, there may be a significant thermal influence at the gage-face. Inserting the appropriate geometry, load and creepage values into the thermal equations of Tanvir [17], it is predicted that the temperature rise at the top-of-rail is only about 16 °C, while at the gage-face the calculated temperature rise is between 225 and 675 °C, depending on the friction coefficient applied there. As discussed in Ref. [18], the fric-

tion coefficient between metals generally decreases with sliding speed.

### 3.4. Lateral forces and wheel climb

A key concern for passenger railways is the presence of high lateral forces and the resultant effects on the safety and economics. From the perspective of safety, high lateral forces:

- Exacerbate the potential for wheel climb. The relationship between lateral forces and wheel climb has been well explained by many authors (e.g. [19,20]).
- Increase the amount of rail roll, and can lead to a rail rollover derailment on poor track. This is primarily a concern on spiked track where the rollover restraint due to fasteners has effectively evaporated. Most passenger systems, since they have elastically restrained track and relatively low axle loads, do not face rail rollover as a significant concern.

From an economic view, high lateral forces are problematic because they:

- Increase the contact force between rail gauge face and the wheel flange, contributing to high rates of wear.
- Increase the W/R contact stress and the rate of RCF development on both rail and wheel.
- Increase the amount of rail roll, contributing to tie-plate cut-in and fastener deterioration (including broken spikes and clip fatigue).

Fig. 8 plots the  $L/V$  ratios for the lead axles of the power car and coach car, where positive values are for left hand curves and negative values for right hand curves. The  $L/V$  ratio is seen to be roughly the same for the coach and power cars on the high rail, following a 1:1 line. But at the low rail the  $L/V$  values exhibit a distinct difference. At high values (usually sharp curves) the power car and coach car  $L/V$  are roughly the same, but at lower levels (usually mild curves) the  $L/V$  on the power car is, on average, lower than the  $L/V$  on the coach car. This is a direct result of the greater average longitudinal creepages on the powered wheelsets, especially on the high speed, mild curves when the Acela train is nearly always in continuous traction (Fig. 9). These larger longitudinal forces reduce the lateral creep force that can be developed as the wheel/rail contact patch approaches saturation.

With respect the probability of an  $L/V$  wheel climb derailment, we use the wheel climb index derived from Weinstock [19] (see discussion in [21]).

$$WC_{\text{WEINSTOCK}} = \frac{(L/V)_{\text{LOW}} + (L/V)_{\text{HIGH}}}{\text{Nadal limit} + \mu_{\text{LOW}}}$$

where the well-known Nadal limit is given as

$$L/V_{\text{NADAL}} = \frac{\tan \delta - \mu}{1 + \mu \tan \delta}$$

$\delta$  is the maximum contact angle between the high wheel and the rail.

$\mu$  in the Nadal formula is the gage-face friction coefficient and  $\mu_{\text{LOW}}$  the friction coefficient at the top of the low rail. Both are taken to be the upper limit of the adhesion values measured by the instrumented wheelsets (see Fig. 6).

Wheel climb is considered possible for values of the Weinstock index equal to or greater than 1.0.

Substituting in the Acela flange angle of 75° (measured from worn Acela wheels) the wheel climb index can be calculated. The distribution of this index for the four IWS axles is summarized in

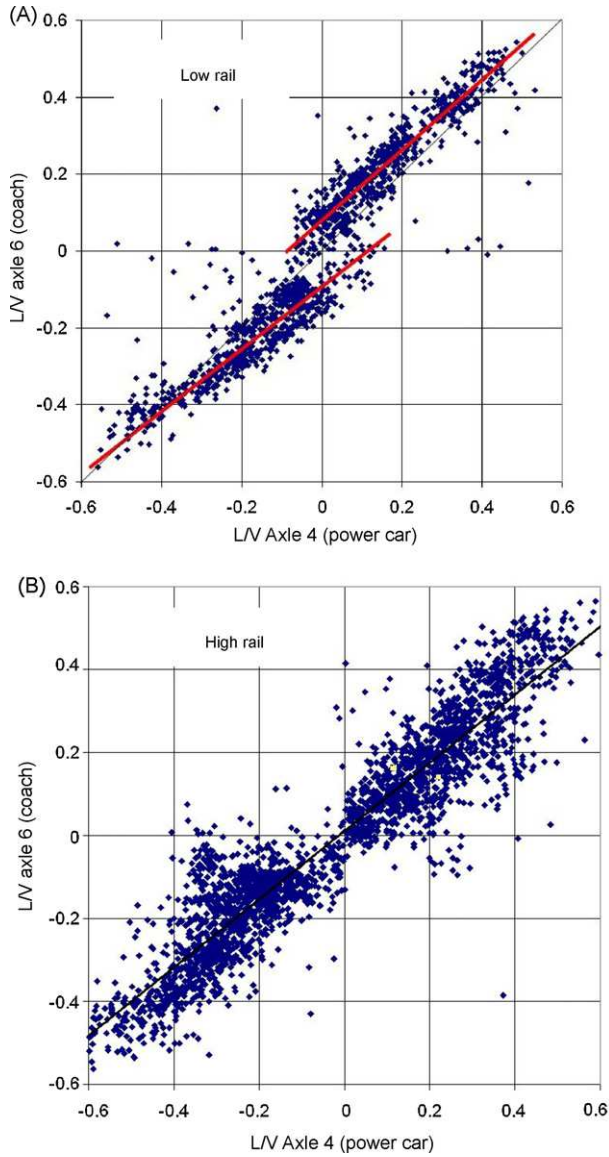


Fig. 8. Lateral/vertical force ratios for the lead axles of the coach and power cars at each point in time.

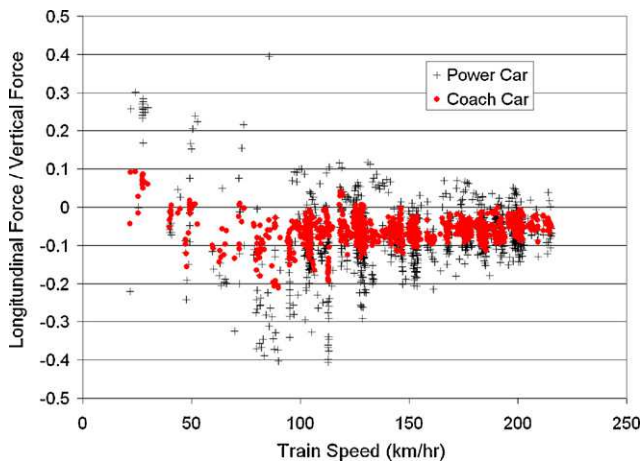


Fig. 9. Longitudinal forces at the low wheel/rail contact are typically higher for the power car than coach car. This allows the coach car to generate higher lateral creepages.

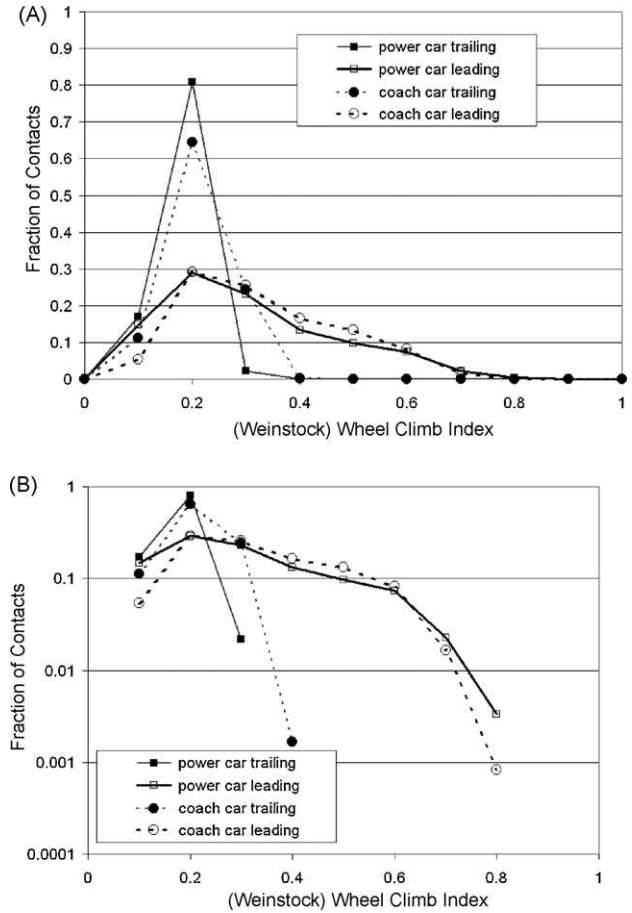
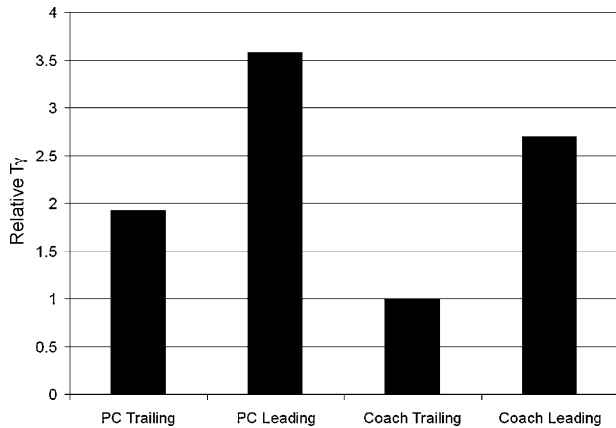


Fig. 10. Wheel climb index (based on a 0.2 s moving average) for the four Acela Instrumented wheelsets. (A) Linear y-axis; (B) logarithmic y-axis.

Fig. 10. For all four wheels, the bulk of the curving conditions result in an index of less than 0.4, i.e. the actual  $L/V$  is less than 40% of the 1.0 level at which a wheel climb might occur, even under these dry conditions. For trailing axles, the wheel climb danger is consistently low. For the leading axle, both coach and power car, the  $L/V$  ratio is occasionally high, with one or two points in a thousand falling between 0.7 and 0.8. The leading axle of the power car shows the highest wheel climb indices.

### 3.5. Rolling contact fatigue and wear

Numerical models of wear and rolling contact fatigue are based on the summation of the so-called  $T\gamma$  index—the product of the traction force and the creepage coefficient [22]. If the modeling of traction force is based on design (or UIC measured) adhesion curves (Fig. 4), the damage index would be significantly underestimated for the dry rail case. Fig. 6 shows that the actual wheel/rail interface tractions that contribute to wear and RCF are up to 2.5 times higher than the design traction values. The instrumented wheelset of course only measures the former, so to assess wear and contact fatigue from IWS data it is necessary to assume that the wheelsets are typically in the linear portion of the Kalker curve, such that the creepage is directly proportional to the traction force. If the interfacial conditions are reasonably consistent, the  $T\gamma$  index is thus proportional to the square of the resolved traction force, i.e.  $wear \propto T^2$ . Summing the values of  $T^2$  for all the low rail contacts suggests that in curves the power cars are responsible for about



**Fig. 11.** Non-dimensionalized summation of  $T^2$  for all low rail contacts on each of the four axles.

60% of the rail damage, and the coach cars the remaining 40% (see Fig. 11).

#### 4. Conclusions

Measurements of vertical, longitudinal and lateral force components from four instrumented wheelsets, two on a power car and two on a coach from the same trainset, were utilized to evaluate adhesion, peak curving tractions, wheel climb index and wear and RCF damage index.

Wheel/rail adhesion utilized by Acela propulsion and (regenerative) braking system is limited in tangent track by the capabilities of the propulsion system. The measured adhesion follows the designed characteristics of the traction and braking system.

The peak traction on dry rail under saturated creepage condition was established from the measurements of wheel/rail creep forces at the inner wheels when in curves. The peak tractions are constant at about 65% until approximately 90 km/h and then drop off with speed. At a speed of 200 km/h the measured peak traction is 22%. These values are higher than those typically used in most modeling efforts and can be expected to have a significant impact on any safety, ride quality or wheel/rail damage calculations modeled.

Numerical simulation of the Acela coach car found that in order to get good agreement with the forces measured while negotiating a 1750 m radius curve at 200 km/h, the friction coefficient needed to be set to a value below 0.3, which is less than half the low speed friction coefficient.

Propensity to derailment was calculated from the measured values of tractions at all four wheelsets using an index based on work by Weinstock. The leading axle of the power car exhibited slightly higher values of this index, though all were well below 1.0, the level above which the  $L/V$  wheel climb is probable.

The wear and RCF damage was evaluated using the product of traction force and creepage coefficient, the so-called  $T_y$  index. Based on this index, power car wheelsets account for about 60% of the wear and RCF damage to rails and wheels in curves, with the coach car wheelsets being responsible for the remaining 40%.

#### Acknowledgments

The authors are grateful for the various contributions of Dr. Kevin Sawley (NRC, now Interfleet) for his many challenging questions, Mr. Frank Grabowski (LTK) for his assistance in understanding power control systems, Dr. Yan Liu (NRC) for undertaking the NUCARS modeling work, and Messrs Brian Whitten and Eric Sherrock (ENSCO) for assistance in translating the instrumented wheelset data.

This work was performed as part of a study funded by the US Federal Railroad Administration, contract #DTFR53-01-H-00304. The support of the FRA, and especially Dr. Magdy El-Sibaie, is gratefully acknowledged.

#### References

- [1] S. Mace, et al., Effect of wheel and rail profiles on gage widening behavior, in: Proceedings of the ASME/IEEE Joint Railroad Conference, Chicago, 1994.
- [2] Instrumented wheelset system results verified the high speed safety standards, FRA Research Results RR00-05.
- [3] D. Li, S. Kalay, W. Shust, Vehicle/track interaction tests of three freight vehicles on revenue service tracks, ASME RTD 21 (2001) 17–23.
- [4] A. Pak, A. Kendrick, Use of Instrumented Wheelset to Quantify Coal Car Performance Under Increased Axle Load Conditions, Transportation Development Centre, Montreal, 1996.
- [5] D. Ahlbeck, H. Harrison, Techniques for measurement of wheel-rail forces, Shock Vib. Digest 12 (10) (1980).
- [6] A. Berghuvud, A. Stensson, Prediction of lateral wheel–rail contact forces for ore wagons with three-piece bogies, in: Proceedings of the Mini-conference on Vehicle System Dynamics, Identification and Anomalies, Technical University of Budapest, Budapest, Hungary, 1998, pp. 161–170.
- [7] K. Lewis, R. Jackson, D. Carter, Qualification and acceptance testing of a high-speed passenger locomotive using instrumented wheelsets, ASME RTD 26 (2003) 157–165.
- [8] M. Fermer, J. Nielsen, Vertical interaction between train and track with soft and stiff railpads—full-scale experiments and theory, Inst. Mech. Eng. F: J. Rail Rapid Transit. 209 (1) (1995) 39–47.
- [9] M. Godet, Third-body approach: a mechanical view of wear, Wear 100 (1984) 437–452.
- [10] J. Kalousek, et al., The Benefits of Friction Management—a third body approach, presented at the World Conference on Railway Research, Colorado Springs, Colorado, 1996.
- [11] K. Hou, et al., Thermal effect on adhesion in wheel/rail interface, in: Proceedings of the 5th International Conference on Contact Mechanics and Wear of Rail/Wheel Systems, July 2000, Tokyo, 2000.
- [12] T. Ohyama, Adhesion characteristics of wheel/rail system and its control at high speeds, in: 4th RTRI Symposium, November 07, 1991, Tokyo, 1991.
- [13] W. Zhang, et al., Wheel/rail adhesion and analysis by using full scale roller rig, Wear 253 (2002) 82–88.
- [14] ORE Report 2, Question B164, “Adhesion during braking, and anti-skid devices”, Utrecht, 1990.
- [15] H.M. Tournay, Rail/wheel interaction from a track and vehicle design perspective, in: IHHA 1999 STS—Conference Wheel/Rail Interface, Moscow, 1999.
- [16] J. Kalousek, Wear and contact fatigue model for railway rail, NRC Technical Report, TR-WE-50, NRC No. 27491, TDC No. TP8344E, October 1986.
- [17] M.A. Tanvir, Temperature rise due to slip between wheel and rail—an analytical solution for hertzian contact, Wear 61 (2) (1980) 295–308.
- [18] N. Saka, A.M. Eleiche, N.P. Suh, Wear of metals at high sliding speeds, Wear 44 (August) (1997) 109–125.
- [19] H. Weinstock, Wheel-climb derailment criteria for evaluation of rail vehicle safety, Paper no. 84-WA/RT-1, Winter Annual Meeting of the American Society of Mechanical Engineers, November 1984.
- [20] H. Wu, J. Elkins, Investigation of wheel flange climb derailment criteria, TTCI report number 931, 1999.
- [21] E. Magel, Development and application of a wheel-climb ‘index’, NRC report CSTT-RVC-TR-098-DRAFT, July 2005.
- [22] G. Donzella, et al., The competitive role of wear and RCF in a rail steel, J. Eng. Fract. Mech. 72 (2005) 287–308.